Sulfide emissions in sewer networks: focus on liquid to gas mass transfer coefficient

Lucie Carrera, Fanny Springer, Gislain Lipeme-Kouyi and Pierre Buffiere

ABSTRACT

H_2S emission dynamics in sewers are conditioned by the mass transfer coefficient at the interface. This work aims at measuring the variation of the mass transfer coefficient with the hydraulic characteristics, with the objective of estimating H_2S emission in gravity pipes, and collecting data to establish models independent of the system geometry. The ratio between the H_2S and O_2 mass transfer coefficient was assessed in an 8 L mixed reactor under different experimental conditions. Then, oxygen mass transfer measurements were performed in a 10 m long gravity pipe. The following ranges of experimental conditions were investigated: velocity flow [0–0.61 $m.s^{-1}$], Reynolds number [0–23,333]. The hydrodynamic parameters at the liquid/gas interface were calculated by computational fluid dynamics (CFD). In the laboratory-scale reactor, the O_2 mass transfer coefficient was found to depend on the stirring rate (rph) as follows: $K_{L,O_2} = 0.016 + 0.025\ N^{3.85}$. A $K_{L,H_2S}/K_{L,O_2}$ ratio of 0.64 ± 0.24 was found, in accordance with previously published data. CFD results helped in refining this correlation: the mass transfer coefficient depends on the local interface velocity u_i ($m.h^{-1}$): $K_{L,O_2} = 0.016 + 1.02 \times 10^{-5}\ u_i^{3.85}$. In the gravity pipe device, K_{L,O_2} also exponentially increased with the mean flow velocity. These trends were found to be consistent with the increasing level of turbulence.

Key words | correlation, gravity pipe, H_2S emission, local turbulence intensity, numerical simulation, reaeration

Lucie Carrera
Fanny Springer
Gislain Lipeme-Kouyi
Pierre Buffiere (corresponding author)
Univ. Lyon, INSA-Lyon, Laboratory of Waste, Water, Environment, Pollution,
9 rue de la physique,
F-69621 Villeurbanne Cedex,
France
E-mail: *pierre.buffiere@insa-lyon.fr*

SYMBOL

a	specific interfacial area ($m^2.m^{-3}$)
a_x	correlation coefficient ($m.h^{-1}$)
b_x, c_x	correlation coefficients (–)
$C_{L,i}$	concentration in liquid phase of component i ($mg.L^{-1}$)
$C_{S,i}$	saturation concentration of component i ($mg.L^{-1}$)
d	stirrer diameter (m)
$D_{m,i}$	diffusivity coefficient of component i ($m^2.s^{-1}$)
d_m	hydraulic mean depth (m)
d_h	hydraulic diameter (m)
Fr_1	Froude number for agitation (–)
Fr_2	Froude number for flow (–)
g	standard gravity ($m.s^{-2}$)
h	the vortex deformation (height $h = h_{max}–h_{min}$) (m)
k	turbulent kinetic energy ($m^2.s^{-2}$)
$K_{L,i}$	overall mass-transfer coefficient of component i ($m.h^{-1}$)
N	stirring rate (s^{-1})
n	coefficient
Re_1	Reynolds number for mixing (–)
Re_2	Reynolds number for flow (–)
Re_i	interface Reynolds number (–)
R_h	hydraulic radius (m)
s	slope ($m.m^{-1}$)
S	wetted surface (m^2)
t	time (t)
u	flow velocity ($m.s^{-1}$)
u_i	weighted velocity at the interface ($m.h^{-1}$)
z	distance (m)

GREEK SYMBOLS

ε	turbulent energy dissipation ($m^2.s^{-3}$)
μ_L	viscosity of water ($Pa.s^{-1}$)
ρ_L	density of the continuous phase ($kg.m^{-3}$)

doi: 10.2166/wst.2017.070

INTRODUCTION

The relation between concrete corrosion and hydrogen sulfide emission was identified more than a century ago. Sulfide is produced by sulfate-reducing bacteria under the form of dissolved H_2S, which can be emitted into the atmosphere. Accumulation of H_2S in the sewer atmosphere in gravity sewer systems is a detrimental phenomenon for several reasons. First, in the presence of oxygen, sulfide is oxidized in sulfuric acid, which is corrosive and causes the disintegration of cement materials. This phenomenon is a real economic loss for communities, because it requires an accelerated rehabilitation and pipe replacement frequency. Second, inhalation of H_2S, even at relatively low concentrations, is toxic to humans. Many deaths during routine maintenance in sewers have been attributed to H_2S toxicity. The sulfide problem will be accentuated in the future because of the temperature increase and the need to expand the cities. Consequently, understanding the fate of sulfide is a major challenge for better management of sewer systems. If the mechanism of sulfide production is quite known, its emission into the atmosphere is less described and deserves more attention (Carrera *et al.* 2015). Since H_2S is produced in anaerobic conditions, the sulfuric cycle is linked to oxygenation. The oxygen concentration in wastewaters and hydrogen sulfide emission both depend on liquid-gas transfer phenomena in sewers (USEPA 1974).

The dynamics of H_2S emission are conditioned by the liquid-gas mass transfer flux. This flux depends, on the one hand, on the difference between the concentration of H_2S in the bulk liquid and the concentration at saturation (given by Henry's law) and, on the other hand, on the mass transfer coefficient and the exchange area. The mass transfer coefficient is, among others, responsible for the dynamics of H_2S concentrations in the sewer atmosphere and has received growing attention; it is now commonly accounted for in dedicated models such as the WATS model (Yongsiri *et al.* 2003). The study of the sulfide liquid-gas mass transfer at laboratory scale and *in situ* is complex due to the hazardous properties of this gas and the lack of sensitive on-line analytical procedures. In addition, accurate methods have to be developed since many phenomena occur simultaneously in real systems, such as H_2S build-up, H_2S biological oxidation, oxygen uptake by microorganisms, etc. As a consequence, the direct determination of mass transfer coefficients in a real sewer is a very difficult task. Two main approaches have been developed in the literature: (i) empirical or theoretical connections between oxygen and hydrogen sulfide transfer coefficients; (ii) empirical models linking the sulfide emission to flow parameters.

The measurement of the mass-transfer coefficient for H_2S is more difficult than for oxygen, because the available measurement methodologies are: (i) the methylene blue method, a sensitive off-line analytical procedure that restrains the sampling frequency and the data acquisition possibilities; (ii) on-line probe, which still lacks data feedback in literature. Consequently, the mass-transfer for H_2S has not been studied in the field and barely at laboratory scale. Therefore, one of the objectives of the present work was to measure the H_2S mass transfer coefficient with an on-line sensor, and to compare it with the O_2 mass transfer coefficient. Theoretically, mass transfer limitations are localized at the liquid side in the laminar diffusion layer, and are related to the diffusivity of the species in water according to Equation (1) (Perry & Green 1985):

$$k_{L,i} \propto D_{m,i}^{0.5} \tag{1}$$

Nevertheless, the exponent 0.5 may not be fully representative of all the hydrodynamic conditions encountered in real sewer networks, and an alternative relation was proposed (Equation (2)), where n is comprised between 0.5 and 1.

$$\frac{K_{L,H_2S}}{K_{L,O_2}} = \left(\frac{D_{m,H_2S}}{D_{m,O_2}}\right)^n \tag{2}$$

Yongsiri *et al.* (2004a, 2004b) experimentally found a constant ratio $K_{L,H2S}$ to $K_{L,O2}$ of 0.86 ± 0.08 at 20 °C. According to the literature, the gas-liquid oxygen mass transfer is strongly influenced by the flow conditions (Table 1). The models gathered in Table 1 were established based on indirect field measurements. These correlations account for the flow, the slope, the pipe geometry and the turbulence level of the system.

Table 1 | Empirical models for gas-water oxygen mass transfer coefficients

Reaeration Estimation Model		
Authors	$K_{L,O_2}\ a$ expression	
Krenkel & Orlob (1962)	$7.235(us)^{0.408}d_m^{-0.66}$	(3)
Owens *et al.*(1964)	$0.222\,u^{0.67}d_m^{-1.85}$	(4)
Parkhurst & Pomeroy (1972)	$0.96(1+0.17Fr_1^2)\,(su)^{3/8}d_m^{-1}$	(5)
Taghizadeh-Nasser (1986)	$0.4\,u(d_m/R_h)^{0.613}d_m^{-1}$	(6)
Jensen (1995)	$0.86(1+0.2Fr_1^2)(su)^{3/8}d_m^{-1}$	(7)

Since the available models (Table 1) estimate global transfer coefficients and refer to parameters depending on the system geometry (d_m, R_h), it would be useful to dispose of models independent of the geometric dimensions of the system. For this purpose, the main idea was to establish a link between the local mass transfer coefficient and local data, collected at the interface, which is basically not related to the size of the system. The objectives of this work were thus:

- to measure the K_L of H_2S and O_2 in the same experimental device in order to estimate the ratio between the two components;
- to compute the local liquid velocities near the interface by computational fluid dynamics (CFD) in order to correlate the measured K_L to the local hydrodynamic parameters;
- to perform a similar analysis in a gravity pipe device by investigating the O_2 mass transfer coefficient and derive a correlation based on local hydrodynamic parameters.

MATERIALS AND METHODS

Mass transfer coefficient K_L in a small reactor

Experimental approach

Batch experiments were performed in an 8 L capacity cylindrical reactor. The temperature was fixed at 20 °C (±0.5 °C) and regulated by water circulation in a water jacket. Stirring was ensured by a Rushton turbine made of four symmetric blades. For all experiments, the stirring velocity N was set between 50 and 140 rpm and controlled by a tachymeter. The calculated dimensionless numbers for stirring were:

$$\text{Froude number } Fr_1 = \frac{dN^2}{g} \tag{8}$$

$$\text{Reynolds number: } Re_1 = \frac{\rho_L N d^2}{\mu_L} \tag{9}$$

The range of values for the stirring velocity corresponds to Reynolds numbers [8,333–23,333] and Froude numbers [0.007–0.015]. Those mixing conditions were chosen to fall in the turbulent flow regime, which intensifies the mass transfer. The vessel had an interfacial area to volume a comprised between 4.73 and 5.11 m^{-1} depending on the surface deformation, which was accounted for by considering the shape of the vortex as a truncated cone. The O_2 mass transfer coefficient was measured according to the conventional reoxygenation method (American Society of Civil Engineers 2003; Capela *et al.* 2004). The experimental procedure consisted of depleting the O_2 content in the liquid phase by adding an adequate amount of sulfite (Na_2SO_3, CAS 7757-83-7) and 1 mg/L of cobalt as a catalyzer ($CoSO_4$, CAS 10026-24-1). O_2 was monitored with an oximeter installed 6 cm under the liquid/gas interface (Mettler-Toledo easySense O_2 21 Oxygen Sensor) and plugged to a computer device and software. The response time of the dissolved oxygen (DO) probe was experimentally checked: during the experimental period it ranged from 25 to 35 seconds, which is far below the duration of the experiment (several hours). The reactor headspace was open to the atmosphere, in order to keep the oxygen concentration constant in the gaseous phase. Based on the two film theory, the oxygen concentration during reoxygenation varied according to Equation (10):

$$C_{L,O_2} = C_{S,O_2}\left(1 - e^{-K_{L,O_2}a\,(t-t_0)}\right) \tag{10}$$

The model was fitted to the experimental data with EXCEL solver. The adjusted parameters were $K_{L,O_2}a$ and $C_{s,O2}$.

For H_2S experiments, the experimental device was isolated from the atmosphere and purged with N_2 to avoid any chemical reaction between O_2 and H_2S, and H_2S accumulation. The determination of the mass transfer coefficient was made on the basis of a degassing technique. The principle was: (i) to create oversaturated conditions by adding a solution of sodium sulfide (Na_2S, $9H_2O$, CAS 1313-84-4) in the liquid phase. The sulfide is mostly in the form of HS^- (at pH >8); (ii) to inject a small HCl drop in order to decrease the pH and to turn HS^- into H_2S, (iii) to measure the decrease in H_2S concentration with the AQUA-MS probe MS-08, composed of an amperometric sulfide probe combined with pH and temperature measurements; (iv) to model the H_2S concentration decrease to determine the mass transfer coefficient. A typical degassing curve for H_2S is shown in Figure 1.

The variation of concentration was supposed to follow an equation similar to Equation (10):

$$C_{L,H_2S} = C_{s,H_2S} + (C_{L,0} - C_{s,H_2S})e^{-K_{L,H_2S}a(t-t_0)}, \tag{11}$$

where $C_{L,0}$ is the concentration at $t = t_0$.

The model was fitted to the experimental results with EXCEL solver, by adjusting $K_{L,H_2S}a$ and $C_{s,H2S}$. Indeed, the theoretical Cs for H_2S should be 0 since the reactor headspace was continuously purged with N_2. Nevertheless, in

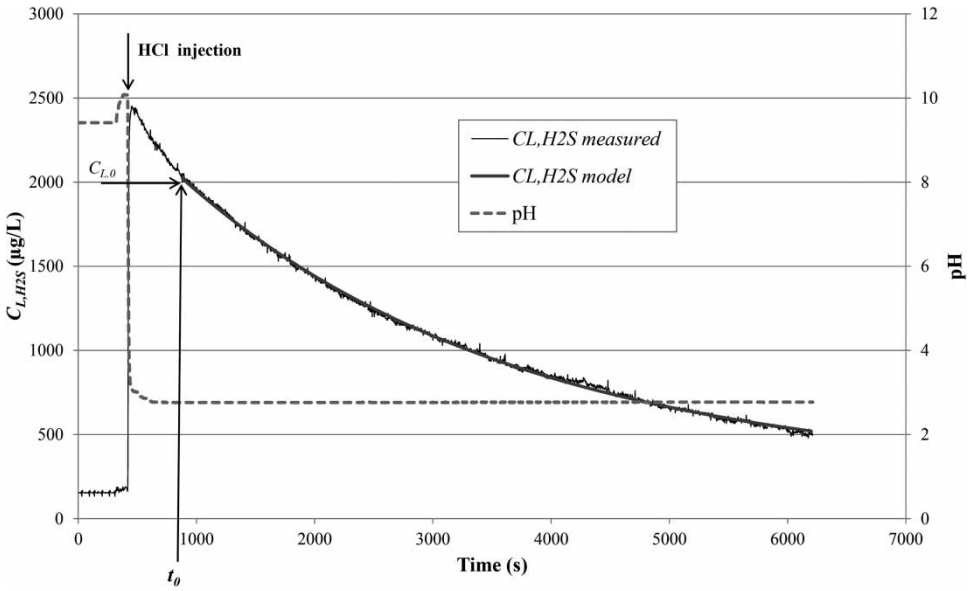

Figure 1 | Typical experimental result for H_2S mass-transfer coefficient determination.

practice the value of 0 did not give consistent results and had to be fitted (fitted values lower than 0.2 mg/L). The aim of this experimental part was to establish an empirical correlation between K_L ($m.h^{-1}$) and the mixing velocity (rph) by means of the ordinary least squares (OLS) method, in the form of:

$$K_{L,i} = a_1 + b_1\, N^{c_1} \tag{12}$$

with a_1, b_1 and c_1 being three distinct constants for O_2 and H_2S. The $K_{L,H_2S}/K_{L,O_2}$ ratio was then determined according to the different hydrodynamic conditions investigated. The results were obtained in clear water (tap water), but could be transferable to real sewers since the ratio between K_L between clear water and wastewater is expected to be known from previous work (Yongsiri *et al.* 2004a, 2004b).

Numerical approach

CFD was used to describe the hydrodynamic conditions near the liquid – gas interface where the mass transfer mainly occurs (Yang & Mao 2014). The ICEM CFD™ was used as a mesh generator, and FLUENT™ v.14 software was used for modeling the flow pattern and the distribution of the liquid and the gas phases along the flow. A two-fluid model with the volume of fluid (VOF) method was used in order to characterize the free water surface. The kε-RNG model was chosen to simulate the gas-liquid turbulence. This model is usually employed to simulate multiphase flow (Paul *et al.* 2004): the kε-RNG model is based on transport equations for the turbulent kinetic energy k and its dissipation rate ε. Furthermore, the effect of swirl on turbulence was included in the RNG model. In the present study, the kε-RNG model was chosen to strike a balance between predictive accuracy and computational economy (CFD On line 2016). The simulation was validated by: (i) the y^+ dimensionless number (between 20 and 100), which accounts for the flow velocity and the turbulent quantities at the nodes adjacent to the solid wall; (ii) the comparison of the experimental free surface deformation with the numerical description of the interface. A difference below 15% would validate our modeling results.

Many meshes had to be envisaged to improve the grid quality and to check that the simulation results were independent of the grid design (Celik *et al.* 2008). The mesh was refined near the impeller blades, the interface and the reactor walls (Figure 2). The mesh quality was specified with an aspect ratio of 22 and an orthogonal quality of 0.69 (Hirsch & Tartinville 2009). The whole 8 L tank was meshed with 4.1×10^5 hexahedral elements. Finally, the O-grid mesh type chosen to model the reactor is presented in Figure 2 in its bottom section.

The numerical model was simulated in steady flow with a RANS turbulence model. The major purpose was to extract the fluid velocity u_i ($m.h^{-1}$) and the Reynolds number Re_i at the interface:

$$Re_i = \frac{\rho_L h\, u_i}{\mu_L} \tag{13}$$

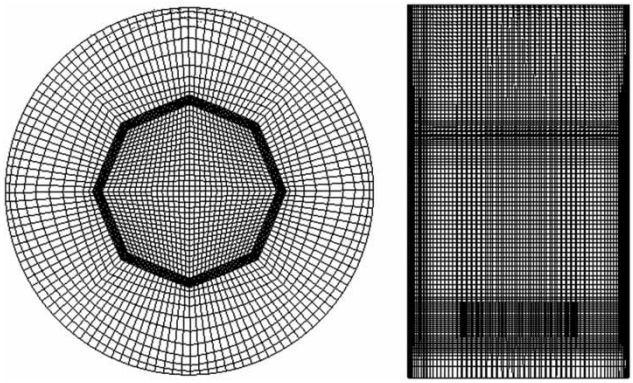

Figure 2 | Computational grid used for the simulations (bottom view at the left and lateral view at the right).

The Reynolds number appeared as the most likely to be extrapolated in a real sewerage system. To represent the interface with accuracy, the vortex deformation (height $h = h_{max}–h_{min}$) was selected to be the characteristic dimension, since it is directly governed by the stirring rate and the interfacial conditions. The local velocity used for the Reynolds number calculation was obtained with numerical results.

Then, it was possible to link K_L to the interface parameters to improve Equation (12) by including the modeling data to obtain Equations (14) and (15) as follows:

$$K_{L,i} = a_2 + b_2\, u_i^{c_2} \tag{14}$$

$$K_{L,i} = a_3 + b_3\, Re_i^{c_3} \tag{15}$$

with u_i the fluid velocity per surface unit ($m.h^{-1}$) at the interface, Re_i the Reynolds number (–), a_2, a_3, b_2, b_3, c_2 and c_3 constants determined by a best-fit regression approach (OLS method). Equations (14) and (15) enable the mass transfer coefficient to be deduced from local parameters describing the interface.

Mass transfer coefficient K_L in a gravity pipe pilot

Empirical approach

The aim of this part was to measure the mass transfer coefficient in a free-flowing pipe system. Oxygen was chosen to investigate the mass transfer coefficient. Experiments were carried out in a 10 m long PVC pipe with an internal diameter of 0.2 m (Figure 3). The slope was adjusted between 0 and 2%. Tap water was pumped from a 2 m^3 tank and the pumping flow was measured by a flow meter (Rosemount 8732 E).

For each experiment, the slope and a constant flow rate was adjusted. Oxygen was depleted below the saturation level in the tank by addition of sodium sulfite. The oxygen concentration (due to reaeration of the liquid phase in the pipe) was measured at steady-state by six oxygen probes (Mettler Toledo easySense O_2 21 Oxygen Sensor) located along the pipe length. The controlled and monitored initial parameters were the water flow rate and the initial dissolved oxygen concentration in the tank. Under each flow condition, the height h and the flow width B were measured. These parameters are sufficient to determine the wetted surface S, the hydraulic diameter d_h and the interfacial area a

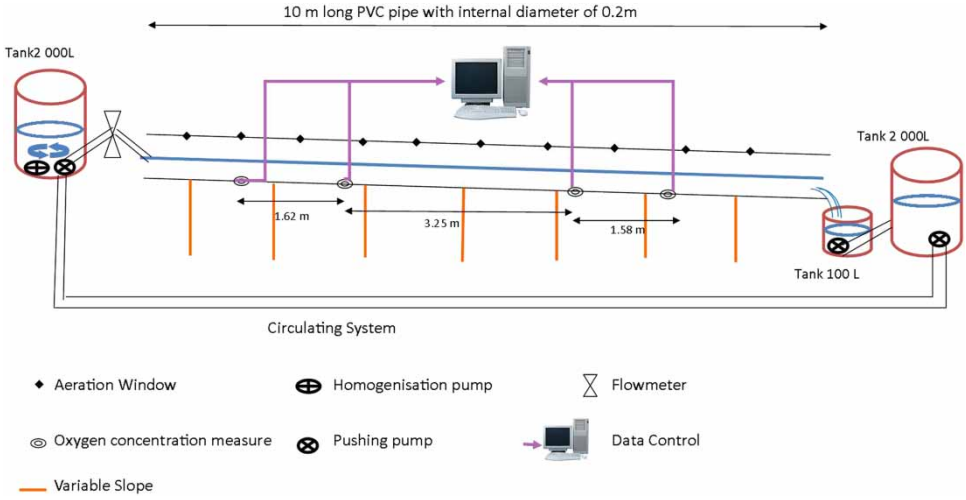

Figure 3 | Gravity pipe device.

(Lahav *et al.* 2004). The turbulence is commonly characterized via Reynolds and Froude numbers following these equations:

$$Re_2 = \frac{\rho_L u d_h}{\mu_L} \tag{16}$$

and

$$Fr_2 = \frac{u}{\sqrt{g d_h}}. \tag{17}$$

In this present work, the flow velocities varied between 0.27 and 0.61 m/s, corresponding to Reynolds number values of [4,332–46,130] and Froude numbers [0.70–0.71].

In steady-state conditions, the mass balance equation reduces to:

$$\frac{dC_{L,i}}{\mathrm{dz}} = \frac{-\mathrm{k_L a}}{\mathrm{u}} \left(C_{L,i} - C_{s,i}\right), \tag{18}$$

where the saturated concentration $C_{s,i}$ is taken from the Winkler table. This equation can then be integrated to calculate the mass transfer coefficient knowing the dissolved concentration $C_{L,i}$. All experiments, in the reactor and in the pipe, were performed at least in triplicate. Within the replicates, outliers were excluded from the dataset by the statistical method of Thompson (Cimbala 2011).

Numerical approach

The system geometry was numerically reproduced. The picturing mesh was refined in the water height value (0.55 to 3.55 cm). The mesh quality was specified by an aspect ratio of 19.9 and an orthogonal quality of 0.66. Two meters of the long pipe were meshed with 1.33×10^5 hexahedral elements (Figure 4). The y^+ value and the orthogonal quality validated the mesh design.

For numerical calculations, the kε-RNG model was chosen to strike a balance between the predictive accuracy and the computational economy. The velocity and the Reynolds number at the interface were obtained with numerical results, in each cell center. The experimental and the numerical oxygen mass transfer coefficient values were compared to validate the modeling results: a difference inferior to 15% would validate our modeling results. Once the numerical description of the flow were obtained, the interface fluid velocity u_i and the Reynolds number Re_i were extracted from the simulated data.

RESULTS AND DISCUSSION

Study of the mass transfer coefficient K_L (O_2 and H_2S) in a small reactor

Experimental approach: link between H_2S and O_2 mass transfer coefficient

Figure 5 plots the hydrogen sulfide mass transfer coefficient ($\mathrm{m.h^{-1}}$) as a function of the stirring rate (rpm) for the dataset obtained in the 8 L reactor (35 experiments). K_{L,H_2S} exponentially increased with the stirring rate. A similar trend was observed for K_{L,O_2} (36 experiments) (results not shown). The exponential evolution of the mass transfer coefficient with the stirring velocity is consistent with the increasing level of turbulence. Indeed, the depth of the liquid film diffusion layer (or the renewal rate of the concentration near the interface) in strongly influenced by the fluid velocity.

The following empirical correlations fitted the experimental results:

$$K_{L,H_2S} = 0.027 + 0.018\, N^{2.98}$$
$$(R^2 = 0.95) \text{ with } N \text{ is in } \mathrm{h^{-1}},\ K_{L,H_2S} \text{ is in } \mathrm{m.h^{-1}} \tag{19}$$

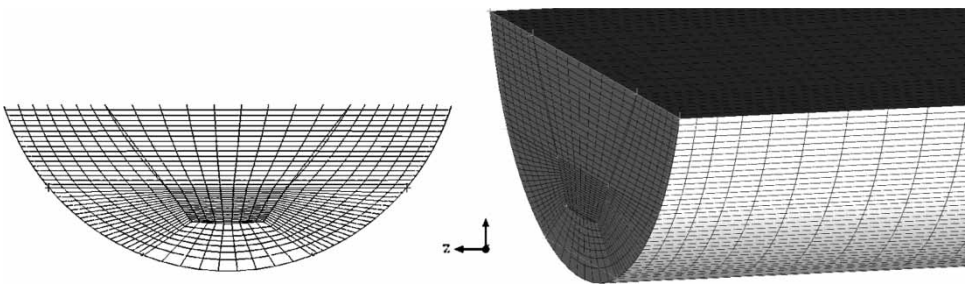

Figure 4 | Computational grid used for the simulations (bottom view at left and lateral view at right) in the pipe.

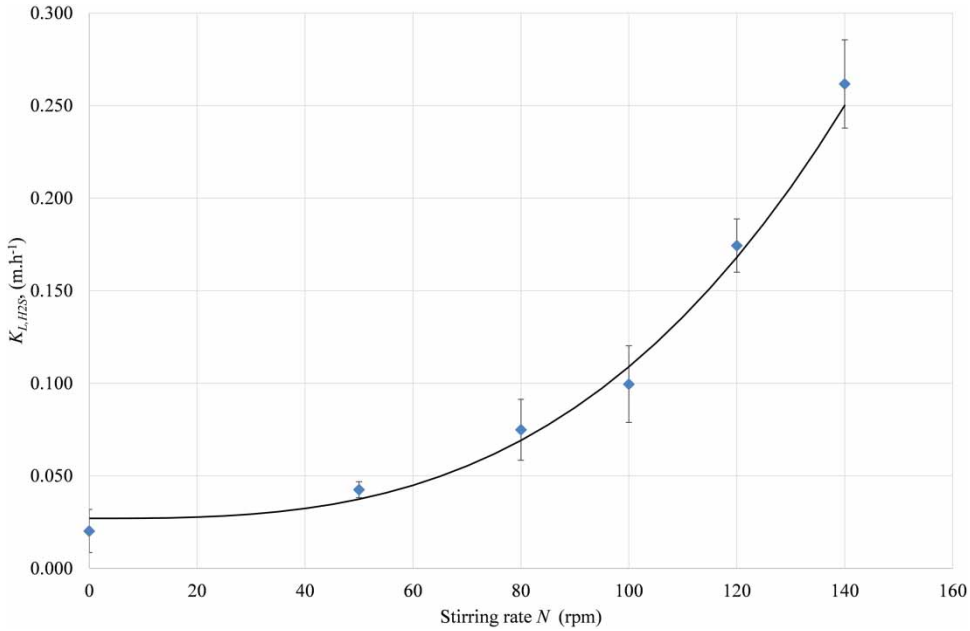

Figure 5 | Influence of the stirring rate mass transfer coefficient of the H_2S (m.h^{-1}).

$$K_{L,O_2} = 0.016 + 0.025\, N^{3.85} \quad (R^2 = 0.90) \text{ with } N \text{ is in h}^{-1}, K_{L,O_2} \text{ is in m.h}^{-1} \qquad (20)$$

The same tendency was observed by Wu (1995), Vasel (2003) and Parkhurst & Pomeroy (1972). Wu (1995) found in aerated bioreactors an exponential trend for the K_La as a function of the stirring velocity, where K_La is proportional to $N^{1.95}$. In rivers and canals, Vasel (2003) found that the mass transfer coefficient was proportional to the square root of the velocity. In sewers, the mass transfer coefficient would be proportional to $u^{3/8}$ (Parkhurst & Pomeroy 1972). Lahav *et al.* (2006) found that the mass transfer coefficient was proportional to the velocity gradient in a sewer pipe. The following step was to study and compare the mass transfer coefficient between the oxygen and the hydrogen sulfide. Figure 6 plots the experimental mean ratio $K_{L,H_2S}/K_{L,O_2}$ as a function of the stirring rate.

The experimental error was symbolized in the figure. The mean ratio was calculated:

$$\frac{K_{L,H_2S}}{K_{L,O_2}} = 0.64 \pm 0.24 \qquad (21)$$

Given the uncertainty, this value falls in the range of the diffusivity ratio ($D_{H2S}/D_{O2} = 0.86$). The rate of the H_2S transfer was generally lower than the reaeration process and exhibits a similar behavior. In 1974, USEPA suggested that the $K_{L,H2S}a/K_{L,O2}a$ ratio was 0.72, which is consistent with our conclusions.

Numerical approach

The modeling results of the flow characteristics in the stirred reactor highlighted no dead zone, and the velocity fields evidenced a homogeneous mixing in the liquid volume (Figure 7). Therefore, the system description is consistent with the basic assumptions needed to apply the two film theory. For the lowest stirring velocity (50 rpm), the local velocities ranged between 0.006 and 0.130 m.s^{-1} (mean value of 0.112). For the highest stirring velocity (140 rpm), the local velocities were modeled in the range of values [0.018–0.341] (mean value of 0.310 m.s^{-1}). The mean velocity modeled in the liquid film was found to be proportional to the stirring rate, with a good accuracy:

$$u_i = 0.0021\, N \ \left(r^2 = 0.97\right), \text{with } u_i \text{ in m.h}^{-1}, \text{ and } N \text{ in rph} \qquad (22)$$

This correlation is fully dependent on the experimental set-up, and therefore extrapolation to other systems is impossible. Nevertheless, it was of interest from a methodological viewpoint. A correlation made from the numerical

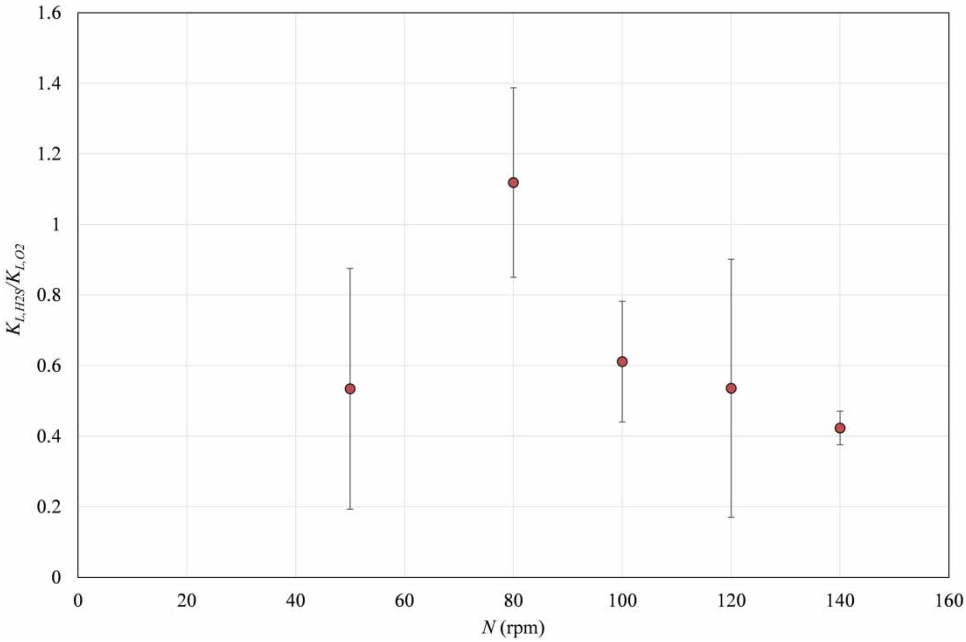

Figure 6 | Influence of the stirring rate on the ratio between the hydrogen sulfide mass transfer coefficient (m.h^{-1}) and the oxygen mass transfer coefficient (m.h^{-1}).

modeling results may be similarly written involving the interface Reynolds number. Those results were then added to the experimental measurements of K_L. For instance, merging Equation (22) with Equation (20) enables the oxygen transfer coefficient to be expressed as a function of the flow conditions at the interface:

$$K_{L,O_2} = 0.016 + 1.02 \times 10^{-5}\ u_i^{3.85} \text{ with } u_i \text{ in m.h}^{-1} \quad (23)$$

with the OLS method, Equation (24) was also edited:

$$K_{L,O_2} = 0.01 + 3.88 \times 10^{-5} Re_i^{1.05} \quad (r^2 = 0.97) \quad (24)$$

Those results make the estimation of the oxygen transfer mass coefficients possible in systems of different geometries, provided that the hydrodynamic conditions are in the same range of values and that local hydrodynamic conditions are accessible with numerical modeling tools as CFD.

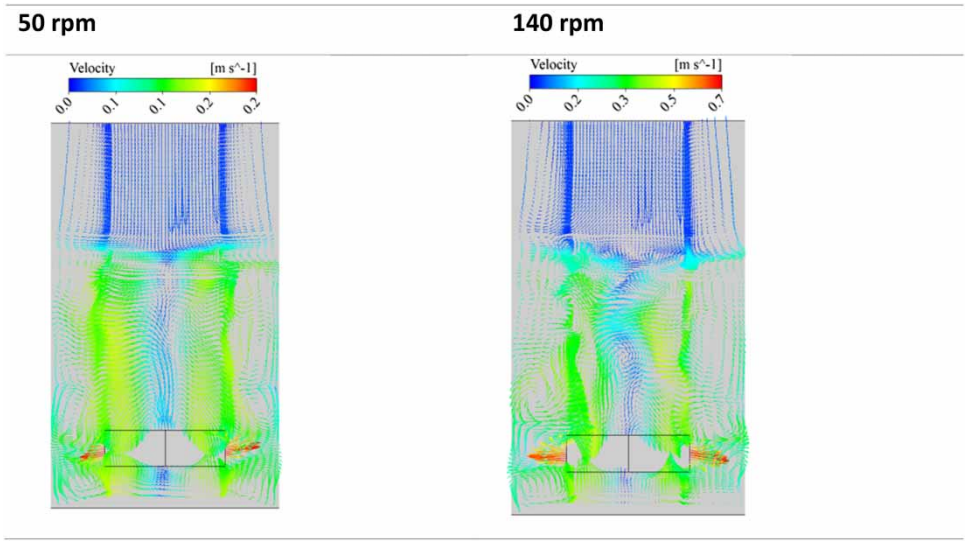

Figure 7 | Velocity fields at 50 rpm and 140 rpm stirring rates (median transverse section).

Study of K_La in gravity pipe with oxygen

Experimental approach

The hydrodynamic conditions in the gravity pipe were determined as follows: (i) subcritical flow, *i.e.* a flow controlled from a downstream point and transmitted in the upstream ($Fr_2 < 1$); (ii) turbulent flow ($Re_2 > 4{,}000$); (iii) no axial dispersion (plug flow). Figure 8 shows that the oxygen mass transfer coefficient $K_{L,O2}$ ($m.h^{-1}$) exponentially increased with the mean water velocity ($m.s^{-1}$). This evolution of the mass transfer coefficient is consistent with the increasing level of turbulence, similarly to what was obtained in the reactor. The $K_{L,O2}$ can thus be derived from the average water velocity (Equation (25)):

$$K_{L,O_2} = 0.117 + 1.77 \times 10^{-11}\, u^{6.58} \quad (R^2 = 0.92) \tag{25}$$

The advantage of this kind of correlation is that it depends on a single parameter, and is easily usable in the field. The K_{L,O_2} values estimated by Equation (25) were in agreement with Parkhurst & Pomeroy (1972), Krenkel & Orlob (1962) and Jensen (1995), with observed mean differences of 42%, 37% and 48%, respectively. Equation (25) can be used for predicting K_{L,H_2S} by applying a coefficient of 0.64 (Equation (21)) in the same range of hydraulic conditions.

Numerical approach

In the gravity pipe device, the simulation results enabled the extraction of the hydraulic conditions at the interface. As in the small reactor, once the simulation grid was designed and approved, and the accuracy of the modeling results verified, the flow was simulated in the pipe. The overall hydraulic patterns were examined. The hydraulic conditions in the liquid-gas boundary layer, the local velocity and the Reynolds number were extracted from the modeling results. The interfacial liquid velocity u_i (averaged over the whole section of the pipe) was found to be proportional to the average velocity ($u_i = 0.92\, u$). Using this result by injecting it in Equation (25) makes the K_L in the pipe predictable from the interfacial velocity:

$$K_{L,O_2} = 0.117 + 3.04 \times 10^{-11}\, u_i^{6.58} \quad (R^2 = 0.92) \tag{26}$$

This predictive correlation is however different from Equation (23), which means that our comparative approach between the two systems (mixed reactor and pipe) needs some refinements in order to obtain a transposable correlation independent of the geometry. Very probably, in free flowing systems another parameter than the average interfacial velocity will have to be accounted for.

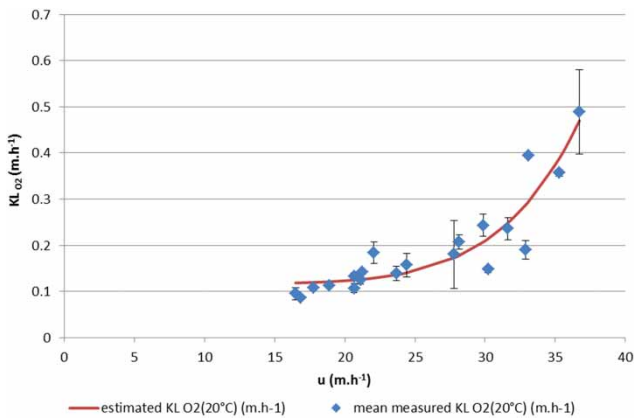

Figure 8 | Flow velocity ($m.h^{-1}$) effect on the oxygen transfer coefficient ($m.h^{-1}$).

CONCLUSION

The dynamics of hydrogen sulfide emission in sewer systems are strongly influenced by the mass transfer coefficient at the interface K_L. This coefficient is known to depend on the flow conditions. The purpose of this work was to collect more data in order to establish a predictive model that could be independent of the system geometry. For this purpose, several scales were investigated: an 8 L mixed batch reactor and a 10 meter gravity pipe device with continuous water flow were set up.

- In the batch reactor, the behavior of the H_2S mass transfer was studied using a new technique based on an on-line sulfide probe as a function of the turbulent conditions (Reynolds range values [0–23,333] and Froude range values [0.70–0.71]). The results were then compared to the O_2 mass transfer coefficient.
- The mean ratio $K_{L,H_2S}/K_{L,O_2}$ was 0.64 ± 0.24, which is consistent with previously reported data.
- K_{L,H_2S} as well as K_{L,O_2} increased exponentially with the flow velocity, in accordance with the increasing level of turbulence near the interface.
- CFD simulations of both systems enabled the proposal of correlations between the mass transfer coefficient and the local interface conditions (Reynolds number at the interface or fluid velocity), so as to make the equations

independent of the averaged hydraulic parameters of the system.

- These results were applied to a gravity pipe. The discrepancy between the measured and the predicted K_{L,O_2} mass transfer coefficients was discussed and the correlations were refined. These equations are expected to be valid in the field and to simplify the modeling and the prediction of the phenomena linked to O_2 and H_2S mass transfer in sewer networks.

REFERENCES

American Society of Civil Engineers 2003 *ASCE Standard Measurement of Oxygen Transfer in Clean Water*. ASCE Library, Reston, VA, USA.

Capela, S., Gillot, S. & Héduit, A. 2004 Comparison of oxygen transfer measurement methods under process conditions. *Water Environment Research* **76** (2), 183–188.

Carrera, L., Springer, F., Lipeme-Kouyi, G. & Buffiere, P. 2015 A review of sulfide emissions in sewer networks: overall approach and systemic modelling. *Water Science and Technology* **73** (6).

Celik, I. B., Ghia, U., Roache, P. J., Freitas, C. J., Coleman, H. & Raad, P. E. 2008 Procedure for estimation and reporting of uncertainty due to discretization in CFD applications. *Journal of Fluids Engineering* **130** (7), 1-4.

CFD On line. http://www.cfd-online.com/Wiki/RANS-based_turbulence_models (accessed 16 January 2017).

Cimbala, J. 2011 Outliers. Presentation, Pennsylvania State University. http://www.mne.psu.edu/me345/Lectures/Outliers.pdf.

Hirsch, C. & Tartinville, B. 2009 Reynolds-average Navier-Stokes modelling for industrial applications and some challenging issues. *International Journal of Computational Fluid Dynamics* **23** (4), 295–303.

Jensen, N. A. 1995 Empirical modeling of air-to-water oxygen transfer in gravity sewers. *Water Environment Research* **67** (6), 979–991.

Krenkel, P. & Orlob, G. T. 1962 Turbulent diffusion and the reaeration coefficient. *Journal of the Sanitary Engineering Division, ASCE* **88** (2), 53–83.

Lahav, O., Lu, Y., Shavit, U. & Loewenthal, R. 2004 Modeling hydrogen sulphide emission rates in gravity sewage collection systems. *Journal of Environmental Engineering* **130** (11), 1382–1389.

Lahav, O., Sagiv, A. & Friedler, E. 2006 A different approach for predicting $H_2S_{(g)}$ emission rates in gravity sewers. *Water Research* **40** (2), 259–266.

Owens, M., Edwards, E. W. & Gibbs, J. W. 1964 Some reaeration studies in streams. *International Journal of Air Pollution* **8**, 469–486.

Parkhurst, J. D. & Pomeroy, R. D. 1972 Oxygen absorption in streams. *Journal of the Sanitary Engineering Division, ASCE* **98** (SA1), 101–124.

Paul, E., Atiemo-Obeng, A. & Kresta, S. 2004 *Handbook of Industrial Mixing: Science and Practice*. John Wiley, New York.

Perry, R. H. & Green, D. 1985 *Perry's Chemical Engineers Handbook*, 6th edn, McGraw Hill, New York, NY, USA.

Taghizadeh-Nasser, M. 1986 Gas-liquid mass transfer in sewers (in Swedish); Materieöverföring gas- vätska I avloppsledningar, Chalmers Teckniska Högskola, Göteborg, Publikation, 3:86 (Licentiatuppsats).

US Environmental Protection Agency 1974 *Process Design Manual for Sulfide Control in Sanitary Sewerage Systems*. US Environmental Protection Agency Technology Transfer Office, Washington, DC, EPA, 625/1-74-005.

Vasel, J.-L. 2003 Aération naturelle dans les procédés d'épuration à biomasse fixée et les écosystèmes aquatiques, *in* M. Roustan, « *Transfert gaz-liquide dans les procédés de traitement des eaux et des effluents gazeux* », Lavoisier Tec & Doc, Chapter 10, pp. 445-488.

Wu, H. 1995 An issue on applications of a disk turbine for gas-liquid mass transfer. *Chemical Engineering Science* **50** (17), 2801–2811.

Yang, C. & Mao, Z. S. 2014 *Numerical Simulation of Multiphase Reactors with Continuous Liquid Phase*, 1st edn. Chemical Industry Press, Elsevier, Oxford, UK.

Yongsiri, C., Hvitved-Jacobsen, T., Vollertsen, J. & Tanaka, N. 2003 Introducing the emission process of hydrogen sulfide to a sewer process model (WATS). *Water Science and Technology* **47** (4), 85–92.

Yongsiri, C., Vollertsen, J. & Hvitved-Jacobsen, T. 2004a Effect of temperature on air–water transfer of hydrogen sulfide. *Journal of Environmental Engineering* **130** (1), 104–109.

Yongsiri, C., Vollertsen, J. & Hvitved-Jacobsen, T. 2004b Hydrogen sulfide emission in sewer networks: a two-phase modelling approach to the sulfur cycle. *Water Science and Technology* **50** (4), 161–168.

First received 14 September 2016; accepted in revised form 24 January 2017. Available online 8 February 2017